

Interactive comment on “Extracting the time variable gravity field from satellite gravity data using a sawtooth filter” by E. Gurria and C. López

E. Gurria and C. López

egurria@fomento.es

Received and published: 10 February 2014

Interactive comment on "Extracting the time variable gravity field from satellite gravity data using a sawtooth filter" by E. Gurria and C.López. Reply to Anonymous Referee #1 (SED 5, C746-C749, 2013), Anonymous Referee #2 (SED 5, C815-C817, 2014) and Anonymous Referee #3 (SED 5, C867-C868, 2014).

We have decided to respond to all three referees in a single text as the individual replies to each referee shared a lot of common ground. Firstly we would like to express our gratitude to all three reviewers for reading the article so thoroughly and contributing with very valuable observations and comments. Our response is divided into two sections: (A) General Comments and (B) Specific Comments.

C984

A. General Comments:

We acknowledge the criticism that our review of filter methods is not complete however our intention was not to present a thorough review but merely to give some examples of filters that have been developed recently. We will add the DDK filter (Kusche 2007, Kusche et al. 2009), the ANS filter proposed by (Klees 2008) and the filter proposed by Swenson (Swenson and Wahr 2006) to our short review.

We chose not to use any of the published filters available because we considered them difficult to implement and we imagine that other Grace users think likewise. We did use the Global Spherical Gaussian Filter and the Spherical Cap Gaussian Filter because it appeared to be the filter most commonly employed by the Grace user community and to our understanding it was the easiest to implement and use of all the filters available. After working with the Spherical Gaussian filter and being thoroughly familiar with its characteristics we can state without a doubt that the Sawtooth filter is simpler to implement and use than the Spherical Gaussian Filter and is a useful instrument for Satellite Potential Field data users.

A second general criticism is that no attempt at a geophysical interpretation of Grace data filtered using the Sawtooth filter is made. We could add an additional example to the text which would serve to show that the amplifying action of the Sawtooth Filter results in recovery of a gravity disturbance which is closer to the true gravity disturbance than the unfiltered, Spherical Gaussian or DDK filtered data. In this sense we have considered the gravity disturbance caused by the recent 11 March 2011 Tohoku-oki Magnitude 9.0 earthquake in Japan and used this as a calibration gravity signal. This calibration signal is obtained by calculating the gravity field disturbance due to the inferred fault plane slip in an elastic earth (Okubo 1992). The fault plane is 625km long, 260km wide with a dip of approximately 10° and a maximum slip on the fault plane of the order of 30 metres (Hayes 2011). We reproduce Hayes' results in figures 1 and 2 to show the earthquake fault slip model but these figures will not be included in the article. Figure 1 shows Hayes' fault slip model for the Tohoku-oki earthquake with a

C985

maximum slip of approximately 30metres. The contours indicate the rupture initiation time in seconds. The earthquake hypocentre is indicated with a star. Figure 2 is the same fault plane displacement projected on the surface and represented on a map of the region. Red lines indicate major plate boundaries. Gray circles are aftershock locations, sized by magnitude. The earthquake fault slip results in a gravity disturbance with an amplitude of approximately 1000 microGal which we present in figure 3 (new figure 7(a) in the article). We consider the Grace observation of this gravity disturbance as registered in the month of April 2011, a few weeks after the earthquake. The static potential used for comparison is the average potential for the year 2009 which is more than a year prior to the earthquake occurrence. We present the Grace UTCSR-GM60RL04 observations of this gravity disturbance in various forms: (i) unfiltered (ii) Gauss Spherical Cap filtered (iii) (DDK1+Gauss Spherical Cap) filtered and (iv) Sawtooth filtered. This is presented in figures 4, 5, 6, 7 and 8 (new figures 7(b), 7(c), 7(d), 7(e) and 7(f) in the article). The DDK1 filtered data were obtained from the ICGM and thereafter filtered by a Gauss Spherical Cap filter. These figures show that both the Gauss Spherical Cap and the (DDK1+Gauss Spherical Cap) filtered Grace observation of the earthquake disturbance is almost two orders of magnitude smaller than the calibration signal whereas the Sawtooth filtered Grace observation is of the same order of magnitude as the calibration signal.

Figures 4, 5, 6, 7 and 8 (new figures 7(b), 7(c), 7(d), 7(e) and 7(f) in the article) present the Net Total Gravity Amplitude which is the difference between the Total Gravity Amplitude minus its corresponding standard deviation. We do this in order to highlight the gravity disturbances which are larger than their error. The colour scale used in the figures indicates negative values in blue tones and positive values in red tones. Those disturbances that lie within the standard deviation will have a negative Net Total Gravity value and will be represented with blue tones while those disturbances that lie above the standard deviation will have a positive Net Total Gravity value and will be represented in red tones. The Total Vector (T), its corresponding Standard Deviation (S) and the Net Total Vector (N) is expressed as:

C986

$$T = [gx^2 + gy^2 + gr^2]^{0.5}$$

$$S = [1 / T] [gx^2 sx^2 + gy^2 sy^2 + gr^2 sr^2]^{0.5}$$

$$N = T - S$$

where:

$gx = (\partial W / \partial X)$ is the derivative along the X axis of the gravitational potential $W = W_3 = (W_2 - W_1)$. Similarly $gy = (\partial W / \partial Y)$ and $gr = (\partial W / \partial R)$.

$sx^2 =$ variance of $(\partial W / \partial X)$. Similarly $sy^2 =$ variance of $(\partial W / \partial Y)$ and $sr^2 =$ variance of $(\partial W / \partial R)$.

N = Net Total Vector.

Figure 7(a) is the Vertical component of the Gravity disturbance caused by the displacement on the fault plane of the 11 March 2011 Tohoku-oki Magnitude 9 earthquake. The fault plane slip was obtained by seismological waveform inversion (Hayes 2011) and the corresponding gravity anomaly was calculated for an elastic earth (Okubo 1992). The resulting gravity disturbance has an approximate amplitude of 1000microGal (1E-05m/s²).

Figure 7(b) is the unfiltered UTCSR-GM60RL04 Net signal namely $N = (T - S)$ where T and S are unfiltered. The data correspond to the month of April 2011 and show the region between 34° North and 45° North and between longitudes 135° East and 148° East. The epicentre of the 11 March 2011 Magnitude 9 Tohoku-oki (Japan) earthquake is indicated by a yellow star. The surface projection of Hayes' fault plane (Hayes 2011) is indicated by a rectangle. The static potential used is the average potential for the year 2009. The scale maximum is 50microGal (5E-07m/s²), which is almost two orders of magnitude smaller than the calibration signal. No clear gravity disturbance due to the earthquake can be identified.

Figure 7(c) is the same data shown in figure 7(b) but now the Net signal $N = (T - S)$ has

C987

been filtered with a Spherical Cap Gaussian Filter with a smoothing radius $r = 600\text{km} = 3\sigma$. The scale maximum is $15\text{microGal} (1.5\text{E-}07\text{m/s}^2)$. A clear gravity disturbance due to the earthquake is visible however its amplitude is two orders of magnitude smaller than the calibration signal.

Figure 7(d) is the Net signal $N=(T-S)$ filtered with a Spherical Cap Gaussian Filter with a smoothing radius $r = 600\text{km} = 3\sigma$ on data that were previously filtered using a DDK1 Filter. The DDK1 filtered data correspond to UTCSR-GM60RL04 available at the ICGM. The scale maximum is $10\text{microGal} (1\text{E-}07\text{m/s}^2)$. No clear gravity disturbance due to the earthquake can be identified.

Figure 7(e) is the original UTCSR-GM60RL04 Net signal $N=(T-S)$ after having been filtered using only the Sawtooth Filter. The scale maximum is $200\text{microGal} (2\text{E-}06\text{m/s}^2)$ and a clear gravity disturbance associated with the earthquake is present. The gravity disturbance amplitude is approximately a factor of five smaller than the calibration signal.

Figure 7(f) is the original UTCSR-GM60RL04 Net signal $N=(T-S)$ filtered only with the Sawtooth Filter but now the data set corresponds to the month of July 2011 which is several months after the earthquake. The scale maximum is $400\text{microGal} (4\text{E-}06\text{m/s}^2)$. The greater amplitude of the disturbance as compared to that observed in the month of April 2011 is most probably due post-seismic deformation.

We have compared the Grace unfiltered and filtered data with a calibration gravity signal. The calibration signal corresponds to Fault Slip in an elastic earth using a totally independent data source namely Seismological Waveform Data measured by seismometers. Figure 7(a) to 7(f) is an important benchmark example that serves to show that the recovered gravity disturbance using a Sawtooth filter on Grace data is of the same order of magnitude as the calibration Gravity disturbance. The gravity field obtained from the Grace Data is a smoothed version of reality with resolution limited by the largest degree used in the harmonic expansion and thus does not compare well

C988

with the very high resolution achieved with a fault model obtained from seismological waveform inversion however what is striking is that the maximum value of the amplitude of the Sawtooth filtered Grace gravity disturbance agrees with the calibration signal to within the same order of magnitude. The unfiltered, Gaussian Spherical Cap filtered and (DDK1+Gaussian Spherical Cap) filtered Grace gravity disturbance is almost two orders of magnitude smaller than the calibration signal. This appears to indicate that the Sawtooth filter provides a Gravity disturbance amplitude which is closer to the true gravity disturbance amplitude than the unfiltered, Gaussian Spherical Cap filtered or (DDK1+Gaussian Spherical Cap) filtered satellite gravity data.

2. Specific Comments:

1. The Sawtooth Filter is simpler than the Spherical Gaussian Filter.

The issue is raised is that the Sawtooth Filter is not simpler to implement and use than the Spherical Gaussian Filter. We are forced to labour the point that the Sawtooth Filter is far simpler to implement and use than the Spherical Gaussian Filter. We have implemented and used both the Global Spherical Gaussian Filter and the Spherical Cap Gaussian Filter and found that prior to processing the satellite gravity data with these filters we had to study the filter characteristics and behaviour. The Spherical Gaussian filter depends on the degree "n" but also on an additional parameter "a" which defines the width of the Spherical Gaussian Filter in the harmonic domain or the equivalent smoothing radius in the spatial domain and the user has to search for the optimum value of the a-parameter or the smoothing radius by trial and error. Further not all smoothing radii are valid as the Spherical Gaussian Filter becomes unstable for large smoothing radii and exhibits "ringing" phenomena in the harmonic domain which can severely distort the data. We have reached the conclusion that the use of the Spherical Gaussian filter is not trivial and requires prior testing and a search of the parameter space before it can be used with confidence whereas the Sawtooth filter is a simple expression that can be used directly and which requires no parameter tuning.

C989

2. The $(\partial W/\partial X)$ component contains very little noise.

We did not include the $(\partial W/\partial X)$ component in figures 1(a) and 1(b) of the article in order to keep the figures simple and focus on the derivation of the Sawtooth filter. We understand that the reader needs to verify the behaviour of all three components and we have thus updated figures 1(a) and 1(b) of the original text (figures 9 and 10 below) showing all three components: $(\partial W/\partial X)$, $(\partial W/\partial Y)$ and $(\partial W/\partial R)$.

3. A query is made as to the determination of the phase shift which leads directly to the formula of the frequency response of the filter. We have shown in Figures 1(a) and 1(b) of the original text that the Radial $(\partial W/\partial R)$ and East-West components $(\partial W/\partial Y)$ are very similar and appear to be shifted in phase. The sine and cosine functions in expressions (1) and (2) in the text are sinusoidal functions with wavelength $L=(\lambda/m)$ for each longitude= λ and each order= m . A shift of $(L/4)$ converts sine terms into cosine terms and cosine terms into -sine terms. If this shift of $(L/4)$ is applied to all the sinusoidal terms in expression (2) then it will have the same sinusoidal terms as (1) and thus will be in phase with (1). This $(L/4)$ shift in all the sinusoidal terms of expression (2) requires a phase shift of $(m\lambda/4)$ within the sine and cosine terms of expression (2) for each longitude= λ and each order= m . Thus:

$$\partial W/\partial Y = -(GM/(r a \cos \varphi)) \sum_n (a/r)^{n+1} \sum_m (-m C_{nm} \sin m\lambda + m S_{nm} \cos m\lambda) P_{nm} \quad (1)$$

$$\partial W/\partial R = -(GM/(r a)) \sum_n (n+1)(a/r)^{n+1} \sum_m (C_{nm} \cos m\lambda + S_{nm} \sin m\lambda) P_{nm} \quad (2)$$

$$\cos (m\lambda + m\lambda/4) = -\sin m\lambda$$

$$\sin (m\lambda + m\lambda/4) = \cos m\lambda$$

$$\partial W/\partial R' = -GM/(r a) \sum_n (n+1)(a/r)^{n+1} \sum_m (C_{nm} \cos(m\lambda+m\lambda/4) + S_{nm} \sin(m\lambda+m\lambda/4)) P_{nm}$$

$$\partial W/\partial R' = -(GM/(r a)) \sum_n (n+1)(a/r)^{n+1} \sum_m (-C_{nm} \sin m\lambda + S_{nm} \cos m\lambda) P_{nm} \quad (3)$$

Now expression (3) is in phase with expression (1).

4. The Potential contains the noise of the $(\partial W/\partial Y)$ and $(\partial W/\partial R)$ components.

C990

The comment has been made that if the $(\partial W/\partial X)$ component is noise free or has low noise then a noise free potential W could be reconstructed from this component. Our response to this is that we thought so too, however the noise is contained in the harmonic coefficients used to obtain the Potential and thus the noise is also present in the Potential. The derivative of the potential in the X direction results in a low noise signal however the derivatives in the Y and R directions result in signal with noise. We also attempted to obtain additional noise free components from the $(\partial W/\partial X)$ component such as $\partial^2 W/\partial X \partial Y$, $\partial^2 W/\partial X^2$ and $\partial^2 W/\partial X \partial R$ however the noise would re-appear as soon as one performed the derivative in the Y or the R direction.

Another comment is that the observation that the $(\partial W/\partial Y)$ and $(\partial W/\partial R)$ components are similar but out of phase is trivial and can be read off expressions (1) and (2) in the text. The observation that $(\partial W/\partial Y)$ and $(\partial W/\partial R)$ are out of phase might be evident from expressions (1) and (2) however their similarity in amplitude is not evident from (1) and (2) and hence this is not a trivial observation. The components $(\partial W/\partial Y)$ and $(\partial W/\partial R)$ are similar not because the gravity field signal is similar in both components but because the error is similar in nature and amplitude in both components and the error is much greater in amplitude than the gravity field signal. This is the non-trivial observation that has led to the derivation of the Sawtooth filter.

5. An observation is made that the error in the data is not noise as it is not random but rather that the error appears to be systematic. Our response is that the behaviour of the scatter in the data depends on the data window considered. If we consider a single degree and order and compare the variations of the monthly values about the static value then the data appears to be random however if we consider a larger data window which includes the same degree but also all its corresponding orders then the behaviour of the scatter increases with increasing order and this behaviour does appear to be systematic. It is this systematic behaviour which is addressed by the Sawtooth filter.

6. Another issue raised is that the filter does not distinguish between signal and noise.

C991

Our response to this is that it is true that the filter does not distinguish between signal and noise however we show that the noise is associated mainly with the sectorial and near sectorial coefficients and the filter attenuates these coefficients with respect to the remaining Tesseral and Zonal Coefficients.

7. Reference is made to figure 3 to indicate that the error is not only present in the Sectorial and near Sectorial coefficients but also in some Tesseral coefficients. Also that the Sawtooth filter amplifies the signal and the noise and that in so doing the vertical striping noise might be hidden in the amplified noise. Our reply to this is that the Sawtooth filter attenuates the sectorial and near sectorial harmonic coefficients with respect to the tesseral and zonal harmonic coefficients however at the same time it amplifies all harmonic coefficients as a function of degree. This results in a new set of harmonic coefficients and hence a new Potential Field where both the signal and the noise have been modified. We agree that both the signal and the noise are amplified by the action of the filter however at the same time the sectorial and near-sectorial coefficients are attenuated with respect to the remaining tesseral and zonal coefficients. The North-South striping noise is mostly associated with the sectorial and near sectorial coefficients hence the noise and signal associated with these harmonic coefficients is attenuated with respect to the signal and noise associated with the remaining tesseral and zonal coefficients, which do not contain the North-South striping noise. The result is that the remaining signal and noise is amplified by the action of the filter however the North-South striping noise is greatly attenuated.

8. A suggestion is made that the spatial derivatives of the potential W should be expressed in terms of the gravity disturbance and the two deflections of the vertical in the North-South and East-West directions. Our reply to this is that the deflections from the vertical are expressed in terms of an angle and may be more useful for Geodetic applications however in Geophysical applications the vector components of the gravity field are of interest. Satellite gravity data has been used mostly by Geodesists to determine the Geoid and the Gravity field of the earth for use as a Cartographic Reference Frame

C992

however the authors believe that the use of the time variations of the gravity field will be used mainly for Geophysical studies and hence the vector description of the Gravity field will be more useful.

9. An objection is made to the term "dispersion" as used in the text. To this the authors reply that they were using the term qualitatively to refer to the scatter of the data without considering the formal quantitative definition of the term as used in some texts on Probability and Statistics. The use of the term "dispersion" will be substituted by the term "scatter" when referring qualitatively to the uncertainty in the data.

10. A query is made as to the use on Page 1879 of the numerical labels such as 10152181. The numerical labels used are shorthand notation to indicate year/start-day/end-day of the monthly data set, hence the label 10152181 indicates the following: year=2010/start-day=152/end-day=181. We agree that June 2010 would be more conventional and the figures will be modified using the labeling convention month/year to make the text clearer.

11. The title in Figure 3(b) of the article should indicate "Sawtooth Filter" instead of "Global Gauss Filter". This was an erratum. Thank you.

12. Identification and Characterisation of the Error.

We characterise the error in the harmonic coefficient data by showing two aspects of the nature of the error: (i) the scatter of the monthly harmonic coefficients about the yearly mean and (ii) the corresponding standard deviation. The monthly harmonic coefficients contain the time variable signal and the average of these same coefficients over a whole year will retain some of the time variable signal however we observe that the time variable signal is much smaller than the error. The scatter about the mean value is visually informative and has been used only to characterize and describe the nature of the error qualitatively. The corresponding standard deviations quantify the error about the mean which we use as a reference or static field for comparison with the monthly solutions. The error in the monthly solutions is that given by the data provider

C993

of the UTCSR GM60RL04 data. The difference between the monthly solutions and the static solution results in a set of difference harmonic coefficients and their associated errors are determined using standard error analysis.

13. Cause of the Vertical Striping Noise.

Interest is raised as to the most likely reason for the striping noise. Un-modeled systematic effects such as errors introduced by imperfect reduction of short-time mass motions in oceans and atmosphere, and correlated instrumental effects are suggested. These may be possible causes however we do not attempt to explain the cause of the error but simply to identify its characteristics. We have not attempted to reproduce the error synthetically so we do not have any arguments to explain the origin of the error however we feel that the data density difference between the satellite along-track direction and that between adjacent satellite tracks will affect the inversion process by which the harmonic coefficients are obtained. If we were to attempt to explain the origin of the North-South striping error we would first focus on the data density in the North-South and East-West directions and how it affects the inversion process by which the harmonic coefficients are obtained.

References

- Hayes, G.: Updated Result of the Mar 11, 2011 Mw 9.0 Earthquake Offshore Honshu, Japan, United States Geological Survey, 2011. http://earthquake.usgs.gov/earthquakes/eqinthenews/2011/usc0001xgp/finite_fault.php
- Kusche, J., Approximate decorrelation and non-isotropic smoothing of time-variable GRACE-type gravity field models. *J. Geod* (2007) 81:733-749.
- Kusche, J. Schmidt, R. Petrovic, S., Rietbroek, R. (2009): Decorrelated GRACE time-variable gravity solutions by GFZ, and their validation using a hydrological model. *Journal of Geodesy*, 83, 10, 903-913.
- Klees, R., Revtova E.A., Gunter, B.C., Ditmar, P., Oudman, E., Winsemius, H.C.,

C994

Savenije, H.H.G.: The design of an optimal filter for monthly GRACE gravity models. *Geophysical Journal International* 175, 417-432 (2008).

Okubo S., Gravity and Potential Changes due to Shear and Tensile Faults in a Half-Space. *Journal of Geophysical Research*, Vol. 97, No. B5, Pages 7137-7144, May 10, 1992.

ICGM : <http://icgem.gfzpotdam.de/ICGEM/TimeSeries.html>.

Interactive comment on *Solid Earth Discuss.*, 5, 1871, 2013.

C995

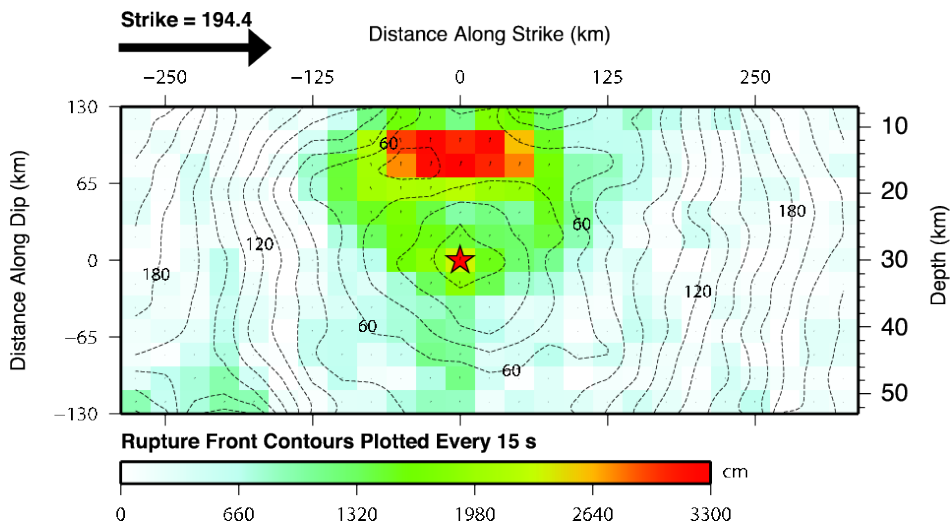


Fig. 1. Not for article: Cross-section of slip distribution of the 11 March 2011 Magnitude 9 Tohoku-oki earthquake. Credit: Hayes 2011.

C996

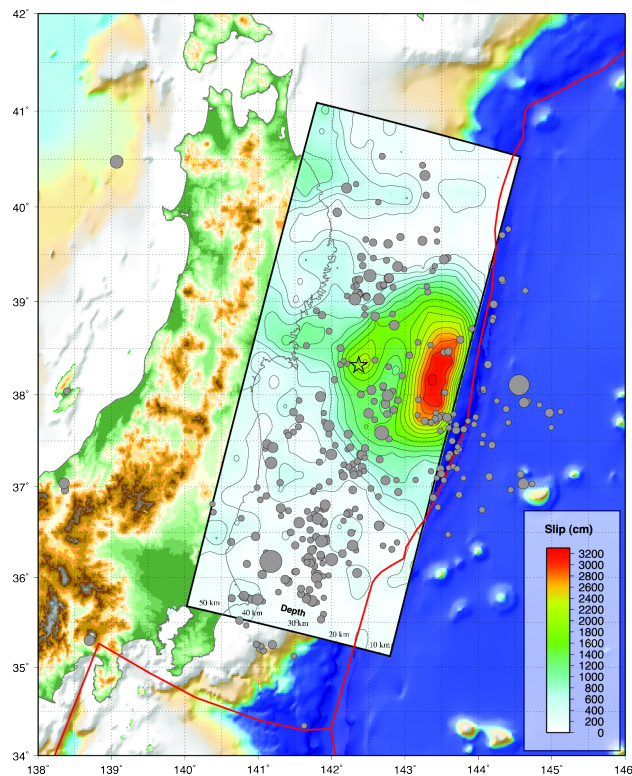


Fig. 2. Not for article. Surface projection of the slip distribution of the 11 March 2011 Magnitude 9.0 Tohoku-oki earthquake. Credit: Hayes 2011.

C997

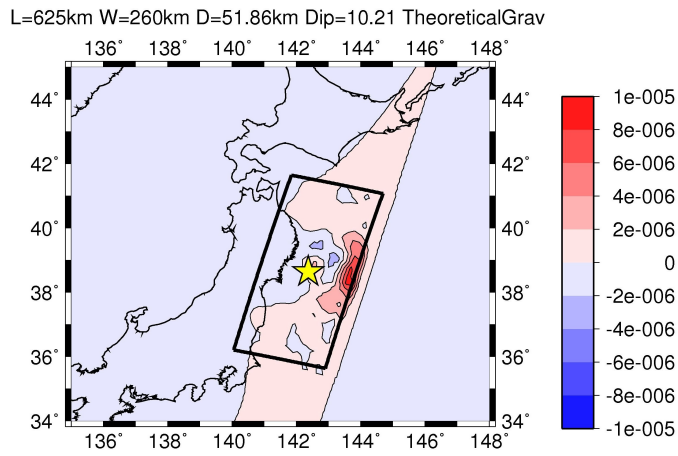


Fig. 3. New Fig 7(a). Calculated Vertical Component of the Gravity disturbance due to Hayes' fault slip model (Hayes 2011) in an elastic earth (Okubo 1992). Maximum amplitude is $1\text{E-}05\text{m/s}^2$ (1000microGal).

C998

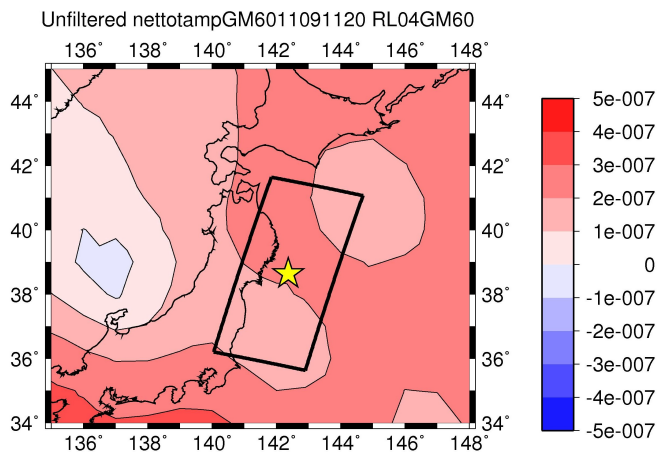


Fig. 4. New Fig 7(b). Unfiltered Net Total Vector (N=T-S) of the Gravity disturbance obtained from UTCSR GM60RL04 for the month of April 2011. Scale Maximum is $5\text{E-}07\text{ m/s}^2$ (50microGal).

C999

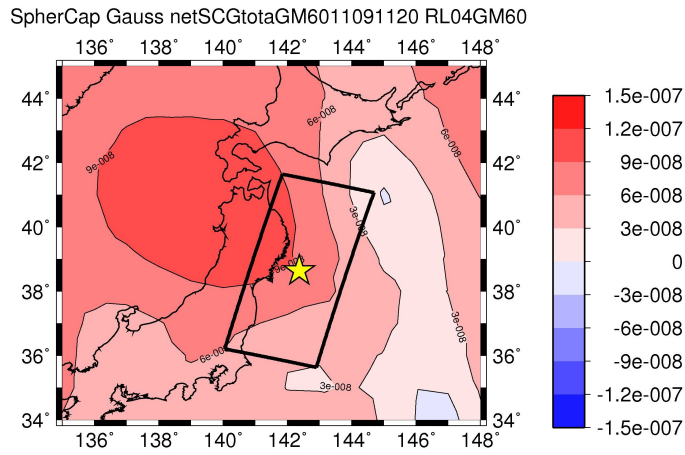


Fig. 5. New Fig 7(c). Gauss Spherical Cap Filtered ($3\sigma=600\text{km}$). Net Total Vector ($N=T-S$) of the Gravity disturbance. Scale Maximum is $1.5E-07\text{m/s}^2$ (15microGal).

C1000

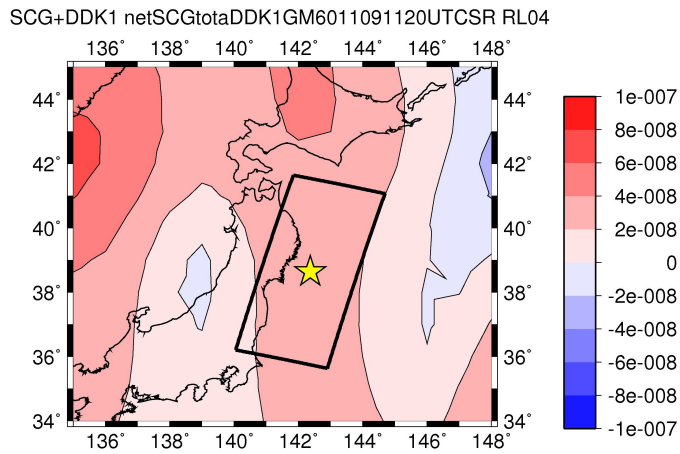


Fig. 6. New Fig 7(d). Spherical Cap Gaussian filter ($3\sigma=600\text{km}$) operating on DDK1 filtered data. Net Total Vector ($N=T-S$) of the Gravity disturbance. Scale maximum is $1E-07\text{m/s}^2$ (10microGal).

C1001

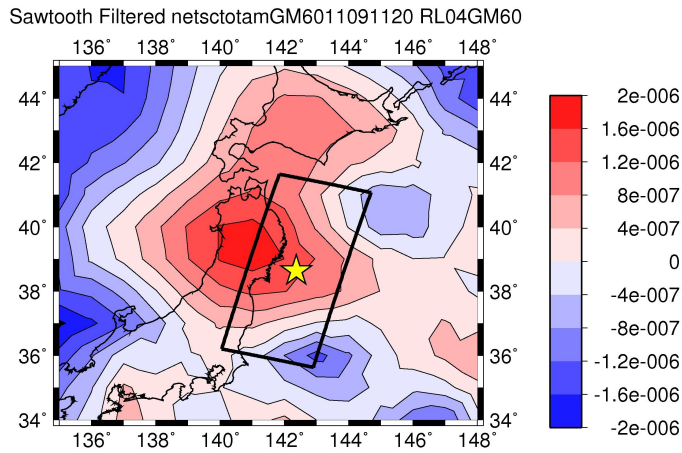


Fig. 7. New Fig 7(e). Sawtooth Filtered Net Total Vector ($N=T-S$) of the Gravity disturbance for the month of April 2011. Scale maximum is $2E-06m/s^2$ (200microGal).

C1002

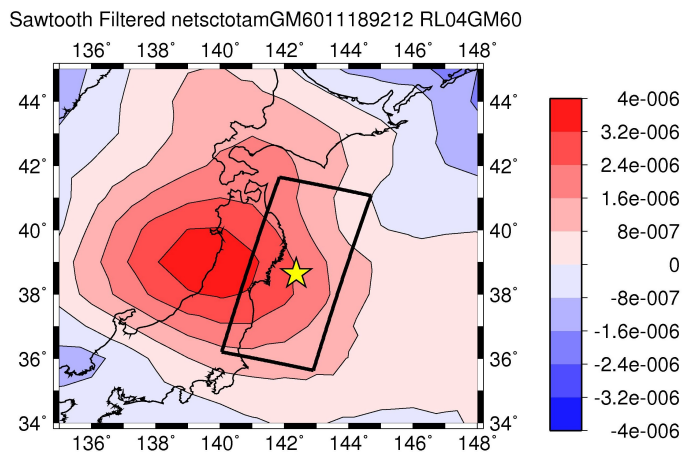


Fig. 8. New Fig 7(f). Sawtooth Filtered Net Total Vector ($N=T-S$) of the Gravity disturbance for July 2011. The scale maximum is $4E-06m/s^2$ (400microGal). The increase can be due to post-seismic deformation.

C1003

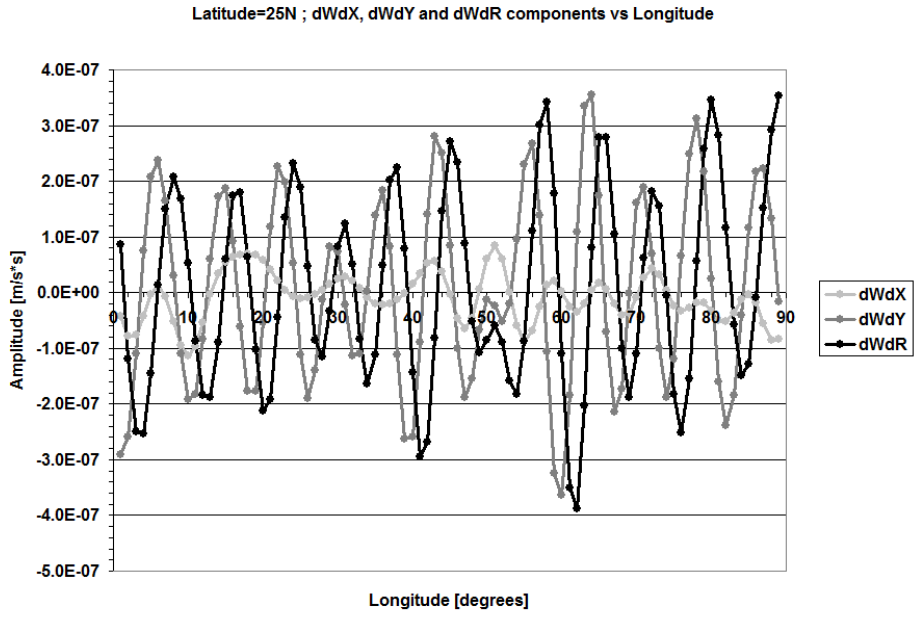


Fig. 9. Figure 1a. Derivatives of the W3 Potential along the parallel with latitude=25°N. The components are: $\partial W3/\partial X$ (light grey), $\partial W3/\partial Y$ (dark grey) and $\partial W3/\partial R$ (black).

C1004

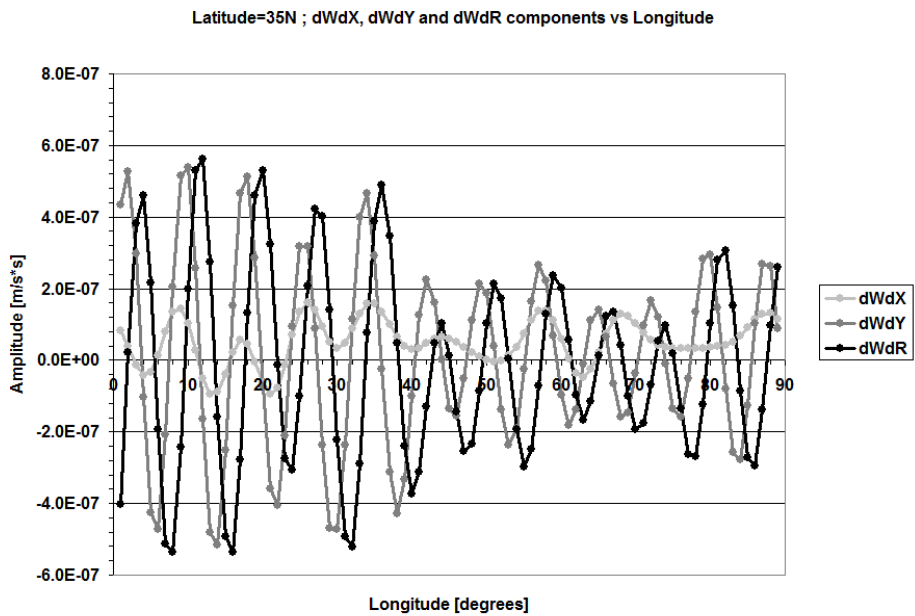


Fig. 10. Figure 1b. Derivatives of the W3 Potential along the parallel with latitude=35°N. The components are: $\partial W3/\partial X$ (light grey), $\partial W3/\partial Y$ (dark grey) and $\partial W3/\partial R$ (black).

C1005